Supplemental Information

Cell PRESS
Open ACCESS

SUPPLEMENTAL REFERENCE

Cohen, G.L., Wright, P.J., DeLucia, A.L., Lewton, B.A., Anderson, M.E., and Tegtmeyer, P. (1984). Critical spatial requirement within the origin of simian virus 40 DNA replication. J. Virol. *51*, 91–96.

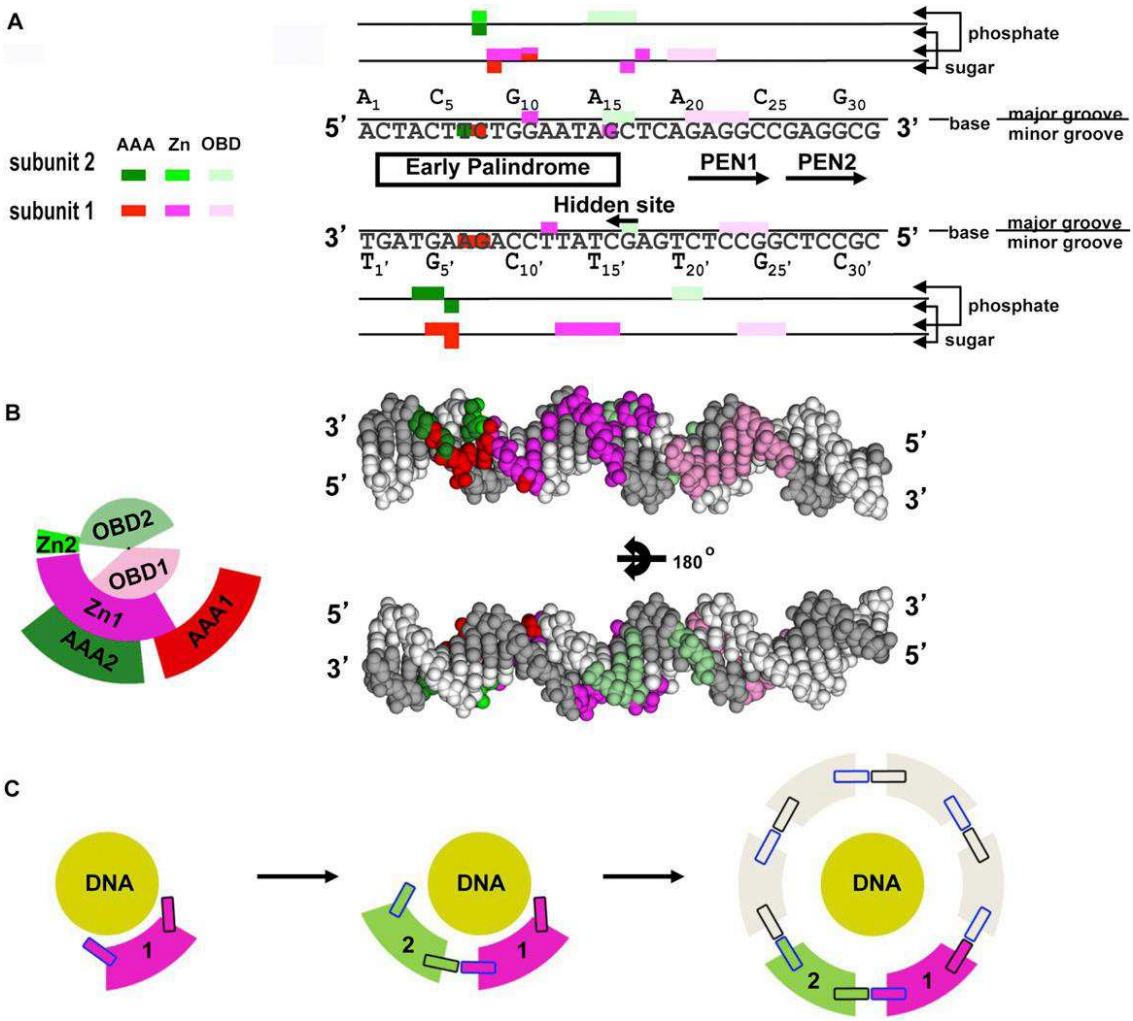

Figure S1. Summary of Interactions between the LTag Dimer and EP-ori DNA, Related to Figure 2

(A) Summary of DNA interactions with subunit 1 domains (colored in pink (OBD1), magenta (Zn1), and red (AAA1)) and subunit 2 (colored in pale-green (OBD2), green (Zn2), and dark-green (AAA2)). Interactions involving the base pairs at the major or minor grooves, sugar moieties, and/or phosphate backbones are indicated on the right side, with color codes indicating specific LTag domains in contact.

(B) Summary of DNA surfaces contacted by different domains of subunits 1 and 2 that are drawn with the same colors as in (A). The cartoon on the left shows the arrangement of the three domains of both subunits in a view along the helix axis of bound dsDNA, which is located between OBD1 (pink) and OBD2 (pale-green). The DNA space-filling model on the right shows surface regions interacting with LTag. Here, no distinction is made between DNA backbone and sugar interactions.

(C) Model of LTag assembly at ori DNA. The first LTag is recruited to the origin through sequence-specific PEN1 recognition by OBD1, followed by Zn and AAA+ domain interactions. This monomer-DNA complex is further stabilized by the additional DNA-interactions made by some exposed residues on the sides of the subunit, such as K271 and N515, that are buried when interacting with other subunits (first panel). When the second LTag is recruited to the origin, which is mediated by the weaker OBD2-hidden site, those originally exposed residues are now at the interface with the incoming subunit, and will switch from DNA-binding to protein-binding (middle panel). Continued recruitment of LTag subunits will repeat this process, and a ring will be formed when all six subunits are recruited.

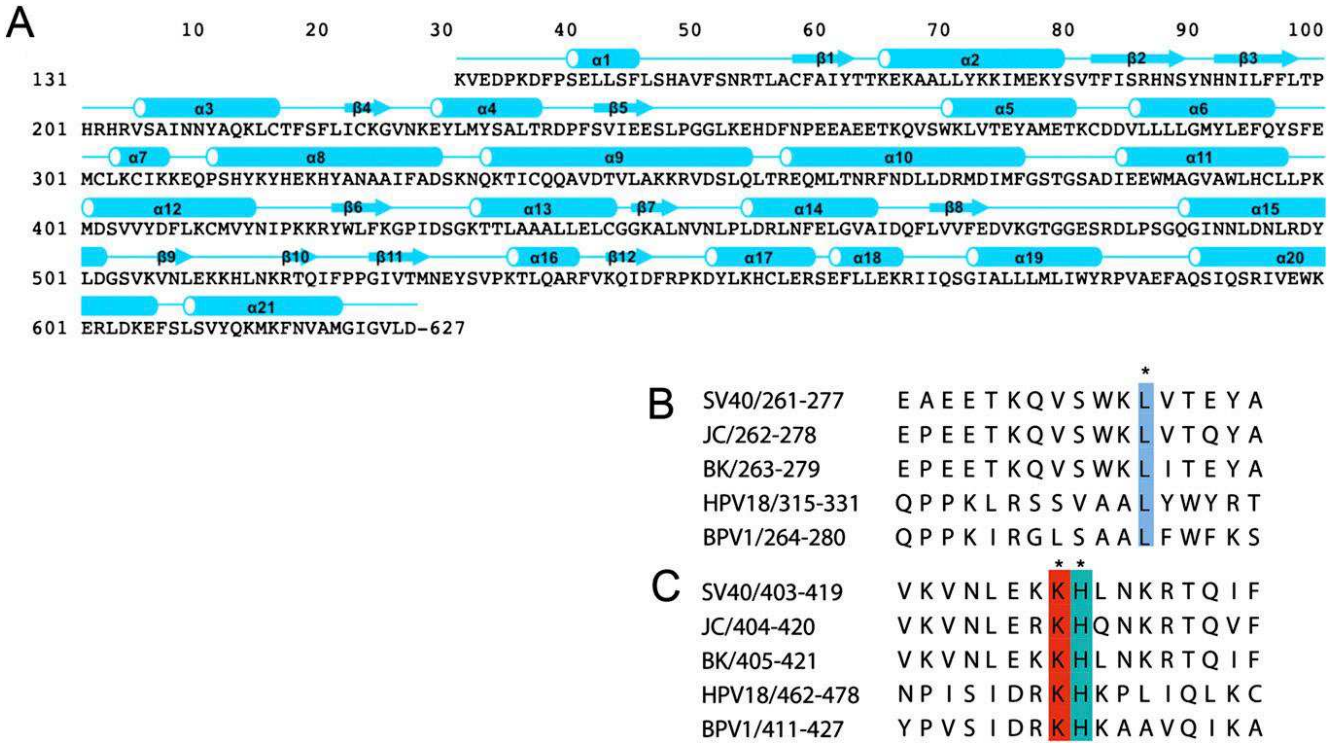

Figure S2. Secondary Structure of SV40 LTag131-627 and Sequence Alignment in the Region of K271 and K512/H513, Related to Figures 2 and 3

(A) Secondary structure of SV40 LTag131-627 that contains the OBD, Zn domain and AAA+ domain in the LTag-ori DNA complex. Arrows represent β strands, bars denote α helices.

(B and C) Multiple sequence alignment around K271 (B) and K512/H513/N515 (C). The alignments show that K512 and H513 are absolutely conserved in polyomaviruses and the distantly related E1 helicase of papillomaviruses. K271, N515 are highly conserved only in polyomaviruses, but not in E1. Alignment was done using the alignment tool T-Coffee and viewed using Jalview.

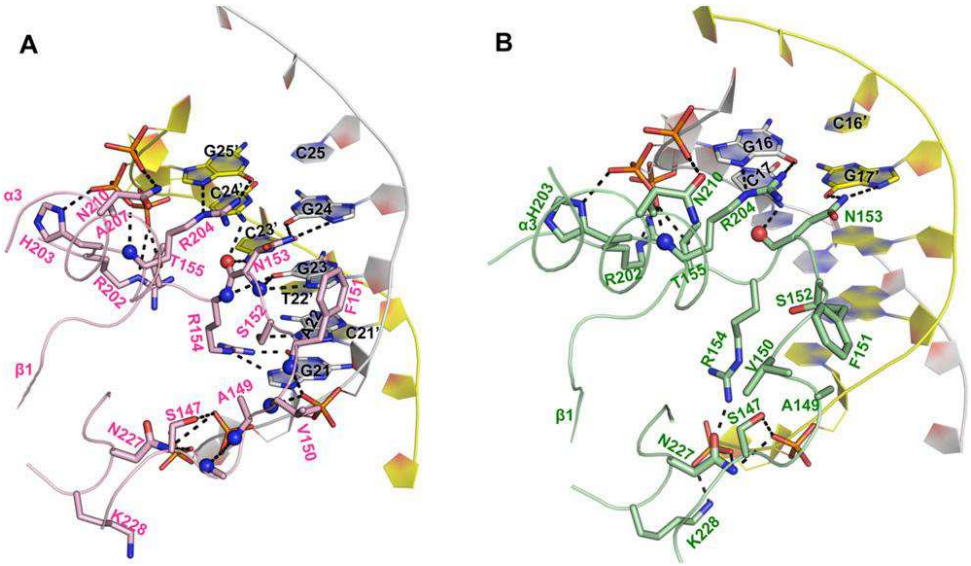

Figure S3. More Detailed Interactions between the Two OBDs and ori DNA, Related to Figure 3

(A) Detailed interactions between OBD1 and PEN1.

(B) Detailed interactions between OBD2 and the hidden-site that is next to PEN1 but more distal to PEN2 (see Figure 1B).

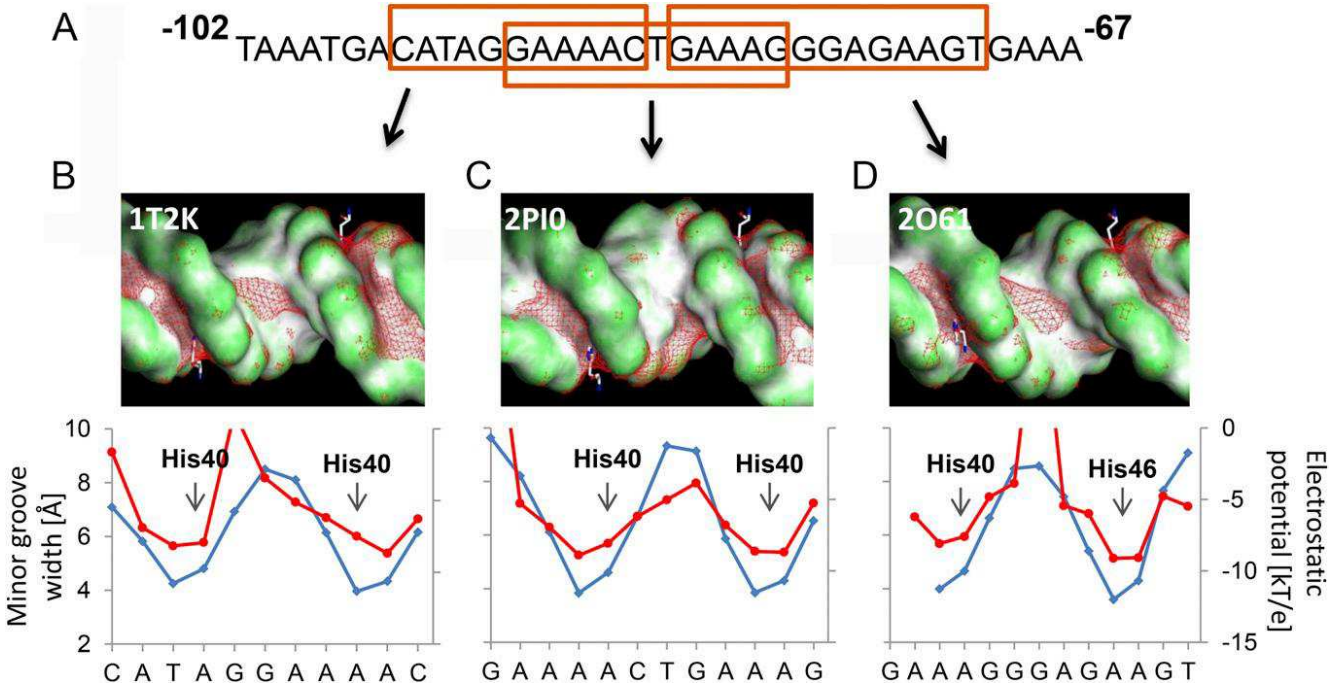

Figure S4. Minor-Groove Shape Readout through Histidine Residues Observed in the IFN-β Enhanceosome, Related to Figure 4

(A) DNA sequence of IFN-β enhanceosome with boxes indicating three different crystal structures containing different overlapping parts of the multiple interferon regulatory factor (IRF)-DNA complexes.

(B–D) The minor groove width and electrostatic potential of these three crystal structures have been analyzed and labeled by their PDB IDs: (B) 1T2K (Panne et al., 2004), (C) 2PI0 (Escalante et al., 2007), and (D) 2O61 (Panne et al., 2007). The results show that minor groove width (blue) and electrostatic potential (red) are highly correlated. Histidine residues from IRFs contact minima in groove width and electrostatic potential, namely His40 from IRF-3 and His46 from IRF-7, which are highly conserved residues in IRFs. These His side chains bind DNA alone and are likely protonated due to the highly charged environment of DNA. This observation suggests that histidine can be used to recognize DNA based on a mechanism previously found for arginines and described as shape readout (Rohs et al., 2009, 2010). The initial contact of the LTag AAA+ domain with the ori DNA is formed through this mechanism. Thus, through the analysis of cocrystal structure of LTag and ori DNA complex, together with those of the IFN-β enhanceosome, we have established a histidine-mediated DNA shape-readout mechanism that could potentially be used in the DNA recognition by many protein families.

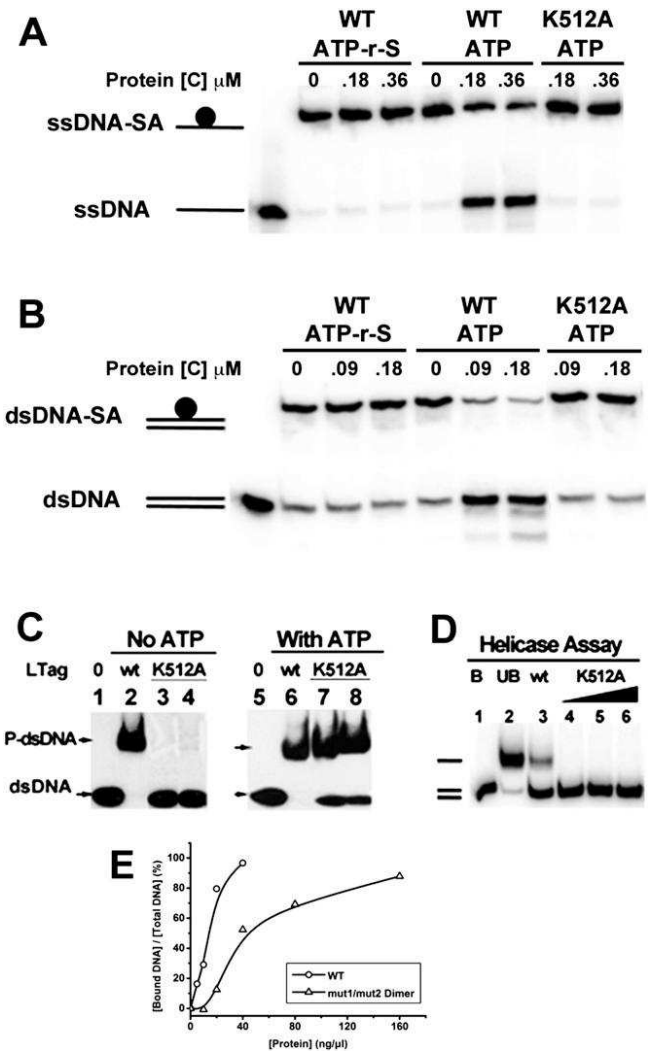

Figure S5. Functional Characterization of the K512A Mutant of the LTag131-627 Construct, and DNA Binding of the Dimer Intermediate Mutant, Related to Figures 3 and 6

(A) Translocation activity on ssDNA of WT and K512A mutant, based on biotinilated ssDNA-streptavidin (ssDNA-SA) displacement assay. Streptavidin (SA) bound to the biotinilated ssDNA can be displaced by WT LTag131-627 only in the presence of ATP. K512A mutant failed to displace the bound SA.

(B) Translocation activity on dsDNA, based on dsDNA-SA displacement assay. The SA bound to the biotinilated dsDNA can be displaced by WT LTag131-627 in the presence of ATP, but K512A mutant failed to do so.

(C) Origin DNA binding assay, showing that K512A did not have detectable dsDNA binding in the absence of ATP, but showed significant amount of dsDNA binding activity in the presence of ATP, possibly because the more stable hexamer formed in the presence of ATP can bind dsDNA readily in the central channel. DNA-binding assays were performed in a 20 μl reaction mix containing 3 pmol WT or K512A mutant (calculated as monomers), 30 fmol of labeled 64 bp origin DNA, and a buffer containing 20 mM Tris (pH 7.5), 100 mM NaCl, 10 mM MgCl2, 1 mM DTT, and 100 mg/ml BSA, with or without 1 mM ATP.

(D) Helicase assay, showing that while WT unwound origin dsDNA, the K512A mutant had no detectable unwinding activity on the origin dsDNA, consistent with the loss of translocation activity of this mutant.

(E) dsDNA binding result for LTag131 WT and mut 1/mut 2 dimer intermediate. In the binding assay, a 146 bp blunt-ended dsDNA that contains the full 64 bp origin sequence was radiolabeled with ^{32}P. DNA binding assay were carried out in a 20μl reaction mix containing 100∼3200 ng of WT or mut 1/mut 2 Dimer, 10∼20 fmol of labeled dsDNA, and a buffer containing 20mM Tris (pH 7.5), 100mM NaCl, 10mM MgCl2, 1mM DTT and 0.1mg/ml BSA, without adding any nucleotide. After incubation at 37°C for 30 min, 5μl of 5x loading buffer (0.1% xylene cyanol, 0.1% bromophenol blue, 50% glycerol) was added. The reaction mixtures were electrophoresed on a 4%∼16% gradient polyacrylamide gel containing 20mM Tris and 30mM cyclohexylaminopropanesulfonic acid (CAPS; pH 9.4) for 50 min at 200V, 4°C. The gels were then dried, autoradiographed and quantified. Bound DNA was quantified using ImageJ and binding curves were prepared with OriginPro. The results clearly showed that the mutant dimer bound the origin dsDNA, even though it showed significantly less binding than WT in the assayed range. For example, at 40 ng/μl protein concentration, ∼100% of dsDNA were bound for WT, but only ∼50% DNA were bound for the mut1/mut2 dimer.

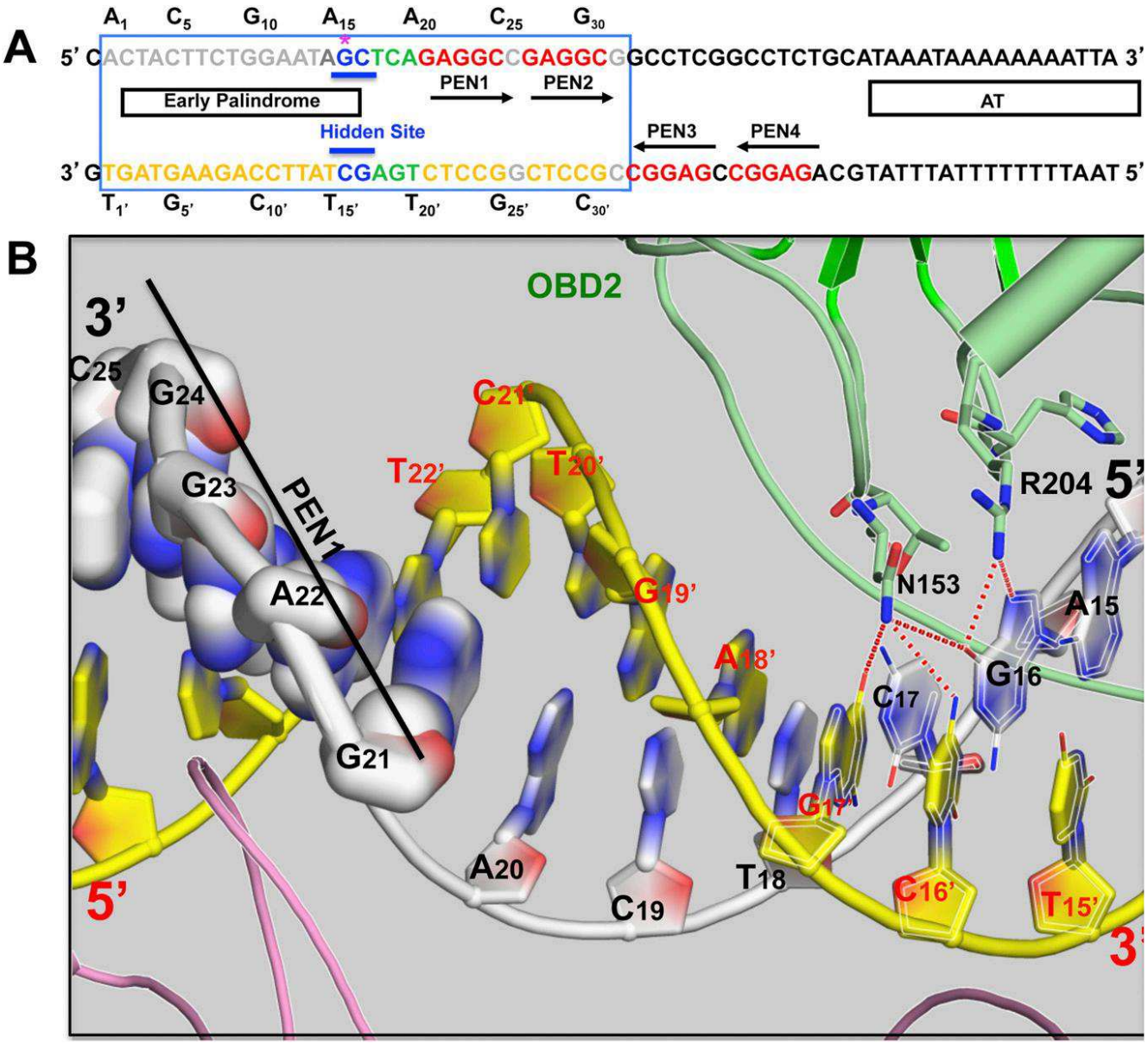

Figure S6. Interactions of LTag OBD2 with the Hidden Site G16C17/C16′G17′, Related to Figure 2

(A) Mutation of the origin DNA sequence showed that the $G_{16}C_{17}/C_{16'}G_{17'}$ dinucleotide (colored in blue) is important for viral DNA replication. It was also shown that the $G_{16}/C_{16'}$ base pair (bp) is more critical than the $C_{17}/G_{17'}$ bp (Deb et al., 1986). The previously identified spacer sequence, $T_{18}C_{19}A_{20}/A_{18'}G_{19'}T_{20'}$ (colored in green), sits between the hidden site and PEN1 ($G_{21}A_{22}G_{23}G_{24}C_{25}$).

(B) The observation that the $G_{16}/C_{16'}$ bp plays a critical role is consistent with the more extensive interactions of OBD2 with the $G_{16}/C_{16'}$ bp compared to the $C_{17}/G_{17'}$ bp (indicated by the more extensive hydrogen bonds with the $G_{16}/C_{16'}$ bp). No interactions of the spacer sequence 5'-TCA with LTag are observed in the structure. Deletion or insertion of the 5'-TCA trinucleotide at this position abolishes viral DNA replication (Deb et al., 1986). Based on the structure, it is conceivable that such deletion or insertion of 5'-TCA would disrupt the spacing between OBD2 binding at the hidden site and OBD1 binding at PEN1, thus disrupting the correct dimer assembly on origin DNA. Moreover, G_{16} of the hidden-site (purple asterisk in A) is protected by LTag binding for dimethylsulphate (Cohen et al., 1984), which is consistent with the binding of G_{16} by LTag OBD2, as the structure revealed that the two reactive atoms of G_{16} in the major groove are forming hydrogen bonds with LTag OBD2 through N153 and R204 (red dashed lines), which should offer the protection. These results indicate that the structural data agree well with previously published genetic and biochemical data. The leading strand is drawn in gray and the reverse strand in yellow in the stick model figure, with 5' and 3' ends labeled.